Published in final edited form as:
Cancer Discov. 2013 March ; 3(3): 338–349. doi:10.1158/2159-8290.CD-12-0313.

Elucidating distinct roles for *NF1* in melanomagenesis

Ophélia Maertens[1,2], **Bryan Johnson**[1,2,¶], **Pablo Hollstein**[1,2], **Dennie T. Frederick**[3], **Zachary A. Cooper**[3], **Ludwine Messiaen**[4], **Roderick T. Bronson**[2], **Martin McMahon**[5], **Scott Granter**[2,6], **Keith Flaherty**[3], **Jennifer A. Wargo**[3], **Richard Marais**[7], and **Karen Cichowski**[1,2,8]

[1]Genetics Division, Department of Medicine, Brigham and Women's Hospital, Boston MA 02115

[2]Harvard Medical School, Boston MA 02115

[3]Division of Surgical Oncology, Medical Oncology and Dermatology, Massachusetts General Hospital, Boston, MA 02114

[4]Department of Genetics, Medical Genomics Laboratory, University of Alabama at Birmingham, Birmingham, AL 35242

[5]Cancer Research Institute & Department of Cell and Molecular Pharmacology, Helen Diller Family Comprehensive Cancer Center, University of California, San Francisco, CA 94143

[6]Department of Pathology, Brigham and Women's Hospital, Boston, MA 02115

[7]The Patterson Institute for Cancer Research, The University of Manchester, Manchester, UK

[8]Ludwig Center at Dana-Farber/Harvard Cancer Center, Boston, MA 02115

Abstract

BRAF mutations play a well-established role in melanomagenesis; however, without additional genetic alterations tumor development is restricted by oncogene-induced senescence (OIS). Here we show that mutations in the *NF1* tumor suppressor gene cooperate with *BRAF* mutations in melanomagenesis by preventing OIS. In a genetically engineered mouse model, *Nf1* mutations suppress *Braf*-induced senescence, promote melanocyte hyperproliferation, and enhance melanoma development. *Nf1* mutations function by deregulating both PI3K and ERK pathways. As such, *Nf1/Braf* mutant tumors are resistant to BRAF inhibitors but are sensitive to combined MEK/mTOR inhibition. Importantly, *NF1* is mutated or suppressed in human melanomas that harbor concurrent *BRAF* mutations, *NF1* ablation decreases the sensitivity of melanoma cell lines to BRAF inhibitors, and NF1 is lost in tumors from patients following treatment with these agents. Collectively, these studies provide mechanistic insight into how *NF1* cooperates with *BRAF* mutations in melanoma and demonstrate that *NF1*-inactivation may impact responses to targeted therapies.

Keywords

RAS; RAF; senescence; NF1; neurofibromin; melanoma; PI3K; mTOR

Corresponding Author: Karen Cichowski, Brigham & Women's Hospital, 77 Avenue Louis Pasteur, NRB 0458C, Boston MA 02115. Phone: 617-525-4722; kcichowski@rics.bwh.harvard.edu.
[¶]current address: Merrimack Pharmaceuticals Inc., Cambridge, MA 02139

There are no conflicts of interest to disclose

SIGNIFICANCE

This study elucidates the mechanism by which *NF1* mutations cooperate with different *BRAF* mutations in melanomagenesis and demonstrates that *NF1*-loss may desensitize tumors to BRAF inhibitors.

INTRODUCTION

Oncogene-induced senescence (OIS) is an irreversible growth arrest that is triggered by a variety of oncogenic signals (1). This form of senescence functions as a protective response to aberrant cell signaling and has been shown to restrict the progression of benign lesions such as melanocytic nevi, lung adenomas, neurofibromas, and prostatic intraepithelial neoplasia (2). Several mechanisms have been proposed to underlie OIS including excessive DNA damage (3–5), heterochromatin formation (6), negative feedback pathways (7, 8), and chemokine signaling (8–10). Notably, these mechanisms are not mutually exclusive and it is likely that they cooperate to establish a senescence response in different tissues.

OIS has been shown to be important for restricting melanoma development in response to activating *BRAF* mutations (11, 12). *BRAF* is mutated in 50–70% of human melanomas (reviewed in (13)). The most frequent *BRAF* mutation ($BRAF^{V600E}$) results in a constitutively active kinase. Analysis of human lesions and mouse models has demonstrated that $BRAF^{V600E}$ mutations drive the development of benign nevi (14–16). However in the absence of additional mutations melanocytes within these nevi ultimately become senescent and do not progress to malignancy (11, 12, 15). Notably, a subset of genetic alterations found in human melanoma prevent BRAF-induced senescence, underscoring the importance of OIS as a mechanism of tumor suppression (15, 17). Nevertheless we still do not have a complete mechanistic or genetic understanding of how OIS is bypassed in melanoma or more generally in cancer.

We have previously shown that oncogenic RAF triggers a potent negative feedback signaling network that suppresses RAS and that this feedback loop plays an important role in OIS *in vitro* (7). Specifically, in response to constitutively activated RAF and MEK proteins, RAS becomes suppressed due to the upregulation of several direct negative RAS regulatory proteins and the concomitant inactivation of positive RAS regulators (7). Moreover RAF-induced RAS suppression substantially attenuates PI3K/AKT signaling, which contributes to OIS in this setting (7). These observations raise the intriguing possibility that mutational events that promote RAS activation might play an important role in preventing RAF-induced senescence. If so, then mutations in such genes might be expected to cooperate with *BRAF* mutations in human cancer.

The *NF1* tumor suppressor gene encodes a RAS GTPase Activating Protein (RAS GAP) neurofibromin, which negatively regulates RAS by catalyzing the hydrolysis of RAS-GTP to RAS-GDP (18). Accordingly, RAS and downstream effector pathways are aberrantly activated in *NF1*-deficient tumors (18–20). *NF1* is mutated in the familial cancer syndrome neurofibromatosis type 1 and has more recently been shown to be mutated or suppressed by proteasomal mechanisms in glioblastoma, lung cancer, and neuroblastoma (21–25); however, the full extent that *NF1* loss may play in sporadic tumorigenesis is unknown. Because of its direct effects on RAS and known involvement in melanocyte biology, we investigated a potential role for *NF1* in melanomagenesis. Our studies reveal distinct mechanisms by which *NF1* mutations cooperate with different *BRAF* mutations in melanomas. Moreover, we have found that *NF1*-loss affects the therapeutic response to BRAF inhibitors.

RESULTS

Nf1 mutations rescue the inhibitory effects of constitutively activated RAF

We previously showed that oncogenic *RAF* alleles potently suppress RAS and subsequent PI3K/AKT signaling and that this suppression is important for OIS in some settings (Fig. 1A) (7). Because *NF1* encodes a direct negative regulator of RAS we reasoned that the

effects of this feedback response might be counteracted by ablating *NF1* expression. Wild-type and $Nf1^{-/-}$ mouse embryonic fibroblasts (MEFs) were stably infected with a hydroxy-tamoxifen (4-OHT) inducible, activated RAF construct (26). 4-OHT substantially suppressed RAS-GTP levels in wild-type cells, consistent with previous findings (Fig. 1B–C) (7). However, RAF activation had minimal suppressive effects on RAS activity in $Nf1^{-/-}$ cells (Fig. 1B–C). Similar effects were also observed in cells in which *Nf1* expression was acutely ablated by shRNA sequences (Supplementary Fig. 1). Shortly thereafter AKT phosphorylation became substantially reduced in *Nf1* wild-type cells at both Ser 473 and Thr 308 (Fig. 1D–E), however *Nf1*-deficiency significantly ameliorated this suppression (Fig. 1D–E). It should be noted that even in the absence of *Nf1*, RAF partially inhibited AKT phosphorylation, consistent with the known involvement of several redundant negative feedback signals (7). Notably, *Nf1*-loss caused a baseline activation of the PI3K/AKT pathway, as previously observed (Fig. 1D–E) (19, 20), and therefore minimized the net suppressive effects on AKT. Most importantly however, RAF activation exerted differential effects on proliferation in wild-type and *Nf1*-mutant cells. Consistent with previous observations oncogenic RAF caused a potent and irreversible growth arrest in *Nf1* wild-type MEFs (Fig. 1F) (27, 28). However, RAF activation did not suppress the proliferation of *Nf1*-deficient cells (Fig. 1G), demonstrating that RAS suppression is a critical mediator of this inhibitory response.

Compound mutations in *Nf1* and *BRaf* promote melanocyte hyperproliferation *in vivo*

To investigate the potential cooperativity of *NF1* and *RAF* mutations in a relevant tumorigenic setting we generated a mouse model to evaluate the effects of *Nf1*-loss in the presence of activating *Braf* mutations. As noted previously *BRAF* is mutated in 50–70% of human melanomas (13). Based on our *in vitro* findings and the fact that neurofibromin plays a well-established role in melanocytes (29), we evaluated the potential cooperativity of *Braf* and *Nf1* mutations in the context of melanomagenesis.

Mice carrying a conditional inactivating mutation in *Nf1* ($Nf1^{flox/flox}$ mice) (30) were crossed to mice with a conditional activating mutation in *Braf* ($Braf^{CA/+}$ mice) (31). These animals were then crossed to a transgenic mouse strain harboring a tamoxifen (TM)-inducible Cre recombinase-estrogen receptor fusion transgene that is under the control of the melanocyte-specific tyrosinase promoter, designated $Tyr::CreER^{T2}$ (32). Activation of CreER by TM in $Tyr::CreER;\ Braf^{CA/+};\ Nf1^{flox/flox}$ mice leads to melanocyte specific conversion of $Braf^{CA}$ to $Braf^{V600E}$ and the conversion of the $Nf1^{flox}$ alleles to *Nf1* null alleles. Six genetic cohorts of animals were generated to evaluate the effects of *Braf* activation in the presence and absence of *Nf1*.

Mice were treated topically with TM 2–3 months after birth as previously described (15). After 4–5 weeks significant darkening of the tails, ears, eyelids, perianal regions, and paws was observed in the $Tyr::CreER;\ Braf^{CA/+};\ Nf1^{flox/flox}$ mice as compared to all other genotypes (Fig. 2A–B). While $Tyr::CreER;\ Braf^{CA/+}$ animals exhibited subtle hyperpigmentation, the skin hyperpigmentation in the $Tyr::CreER;\ Braf^{CA/+};\ Nf1^{flox/flox}$ mice became dramatically more pronounced over time and was concurrent with visible thickening of the respective tissues (Fig. 2A–B). The histopathological features of these lesions were consistent with expansion of the dermis, the skin layer where murine melanocytes reside, and massive melanin deposition (Fig. 2C). An increased number of cells expressing the melanocyte marker S100 was observed, confirming excessive melanocyte hyperproliferation in $Tyr::CreER;\ Braf^{CA/+};\ Nf1^{flox/flox}$ mice as compared to the $Braf^{CA/+}$ genotype (Fig. 2C). Importantly we found that deep dermal lesions derived from control $Tyr::CreER;\ Braf^{CA/+}$ mice stained positive for senescence-associated (SA)-β-galactosidase (Fig. 2D, top panels), as has been shown in human nevi (12) and in lesions within the $Braf^{V600E}$-driven mouse model described by Dhomen et al. 2009 (15). However, senescence

was not observed in *Tyr::CreER; Braf*$^{CA/+}$*; Nf1*$^{flox/flox}$ mice (Fig. 2D, bottom panels). These results are consistent with our cellular studies and indicate that mutations in *Nf1* prevent *Braf*-induced senescence of melanocytes in mice, thereby rescuing the proliferative restriction and triggering excessive proliferation.

PI3K is a well-known effector of RAS (33). We and others have previously shown that *NF1* loss triggers the activation of the PI3K/AKT/mTOR pathway through RAS (19, 20, 34). Moreover, *Nf1* mutations minimize the suppressive effects of *Braf* mutations on this pathway (Fig. 1D–E). Notably, we found that the PI3K inhibitor GDC-0941 prevented the melanocytic hyperplasia in *Tyr::CreER; Braf*$^{CA/+}$*; Nf1*$^{flox/flox}$ mice (Fig. 2E), demonstrating that *Nf1* loss was mediating its effects in melanocytes, in part, by permitting/enhancing the activation of this pathway.

Nf1 and *BRaf* mutations cooperate to promote melanomas in mice

If OIS does in fact restrict tumor development then *Nf1/Braf* mutant mice would be expected to be more prone to developing melanomas. It has been previously reported that a subset of *Braf*^{V600E} mice develop melanomas, presumably due to the stochastic acquisition of additional genetic alterations (15). Consistent with this observation 22% (6/27) of the *Braf*^{V600E} mice in our cohort developed melanomas; however, 57% (16/28) of the *Tyr::CreER; Braf*$^{CA/+}$*; Nf1*$^{flox/flox}$ mice developed melanomas (p=0.008, Chi Square test) (Fig. 3A–E). One *Braf/Nf1* mutant mouse developed two melanomas, which was never observed in *Braf* mutant animals, however melanomas from both genotypes grew at similar rates. These observations support the hypothesis that *Nf1* loss prevents *Braf*-induced senescence *in vivo* and therefore plays a role early in tumor development rather than in progression. However effects on metastasis could not be evaluated in this model, as animals from both genotypes needed to be euthanized due to primary tumor size. While pigmented melanocytes were occasionally observed on the exterior these melanomas were typically hypopigmented (Fig. 3B). All *Braf/Nf1* tumors displayed histological and cytological features typical of malignant melanomas. Tumors were highly cellular with most showing a fascicular growth pattern (Fig. 3C). The degree of pleomorphism was variable. The majority of the tumor cells were amelanotic, however many tumors showed occasional clusters of pigmented cells and pigment containing macrophages (melanophages) (Fig. 3C, right). All tumors involved the dermis as well as subcutaneous soft tissue and ulceration of the tumor surface was seen in the majority of cases. Tumors expressed both S100 (Fig. 3D) and MITF (Fig. 3E), two markers typically used to diagnose human melanomas. Melanomas from both genotypes were further evaluated by immunoblot (Fig. 3F). One tumor that developed in *Tyr::CreER; Braf*$^{CA/+}$*; Nf1*$^{flox/flox}$ mice did not efficiently excise *Nf1*. However in general higher levels of phospho-AKT were typically observed in *Braf/Nf1* mutant versus *Braf* mutant tumors (Fig. 3F–G), consistent with the observation that *Nf1* mutations enhance PI3K/AKT activation and contribute to tumorigenesis, in part, via this pathway (19, 20, 34) (Fig. 2E).

Nf1 mutations desensitize melanomas to BRAF inhibitors

The mutant BRAF selective inhibitor PLX4032 (vemurafenib, Plexxikon/Roche) promotes the regression of human melanomas that harbor activating *BRAF* mutations and has been approved for treating human melanomas (35). To investigate the sensitivity of melanomas harboring compound mutations in *Braf* and *Nf1* to BRAF inhibitors and other targeted agents, we first isolated cells from *Braf* and *Braf/Nf1* mutant tumors. As expected, cells from two independently derived *Braf* mutant melanomas were sensitive to the PLX4032 analogue, PLX4720 (Fig. 4A). However, cells from *Braf/Nf1* mutant tumors were insensitive to this agent (Fig. 4A, IC50>10μM). Biochemical studies confirmed that increasing concentrations of PLX4720 effectively suppressed phospho-ERK levels in *Braf*

mutant cells (Fig. 4B). Notably, however, phospho-ERK was not as effectively suppressed in *Braf/Nf1* mutant cells (Fig. 4B).

Next we evaluated sensitivity to these agents *in vivo*. While allografts from several independent *Braf/Nf1* mutant melanomas were readily established, cells from *BRaf* mutant mouse melanomas never successfully grew as allografts. As such we focused on using *Braf/Nf1* allografts to determine whether we could identify a more effective therapy for these genetically distinct tumors. Two weeks after injection, when tumors were growing in log phase, mice were randomly divided into different treatment groups. Similar to our *in vitro* analysis, *Braf/Nf1* mutant melanomas were relatively insensitive to PLX4720 (Fig. 4C, red) and phospho-ERK was not efficiently inhibited in tumors *in vivo* (Fig. 4D). This finding is consistent with the observation that induction of tumor regression by PLX4032 requires almost complete suppression of ERK signaling (36). In contrast, these tumors were more sensitive to the MEK inhibitor PD0325901 (Fig. 4C, blue), which effectively suppressed phospho-ERK *in vivo* (Fig. 4D). Together with our *in vitro* studies this insensitivity suggests that neurofibromin loss may enhance ERK activity via a BRAF-independent mechanism, which will be discussed further below.

Because our *in vivo* experiments demonstrated that melanocyte hyperproliferation in *Tyr::CreER; Braf*$^{CA/+}$*; Nf1*$^{flox/flox}$ mice could be rescued by the PI3K inhibitor GDC-0941, we evaluated the effects of GDC-0941 on tumor growth, and found that it had a slight growth suppressive effect on these melanomas (Fig. 4C, green). However given that mTOR has been shown to be an important effector in *NF1* mutant tumors we also assessed the mTOR inhibitor rapamycin (20, 34, 37). Rapamycin had a more pronounced effect as compared to GDC-0941, but more importantly it synergized with PD0325901 to promote tumor regression (Fig. 4C, purple). In contrast, rapamycin did not promote tumor regression when combined with PLX4720 (Fig. 4C, violet). Taken together these results suggest that *Nf1* mutations can desensitize *Braf* mutant melanomas to PLX4720. Based on the biochemical function of neurofibromin and the preclinical data presented here, therapies aimed at targeting both MEK and mTOR may represent an alternative therapeutic approach for *Braf/Nf1* mutant tumors.

NF1 is suppressed and/or mutated in human melanoma

Given these compelling mouse phenotypes we next investigated whether *NF1* is lost or mutated in human melanomas. Like p53, neurofibromin can be inactivated by both genetic and proteasomal mechanisms (23). We first evaluated neurofibromin expression in a panel of melanoma cell lines. Four out of eleven cell lines exhibited little or no neurofibromin expression (Fig. 5A). Sequence analysis confirmed that three of these cell lines harbored loss-of-function mutations in the *NF1* gene (Supplementary Table 1). It should be noted that two of the *NF1* alterations (p.K1290K in A375 cells and p.K2307K in WM3670 cells) abolish splice donor sites (c.3870G>A and c.6921G>A, respectively), result in defective splicing and disrupt the *NF1* transcript. Sequence analysis of the cDNA of *NF1* enabled the detection of these aberrant splicing events, however, both *NF1* mutations may have been categorized as ‘non-deleterious’ silent alterations using exome sequencing approaches. We then mined publically available databases and identified numerous additional *NF1* mutations in human cell lines (Supplementary Table 1). Analysis of primary melanomas also confirmed the presence of somatic *NF1* mutations (Supplementary Table 2). In many, but not in all cases, *BRAF* mutations were also present. These findings suggest that while *NF1* mutations can cooperate with activating *BRAF* mutations, they may also play a broader role in melanomagenesis. Interestingly, however, while we expected to find coincidental mutations with *BRAF*^{V600E}, we also observed *NF1* mutations in cells that harbored inactivating *BRAF* mutations (Supplementary Table 1), a point which will be discussed below.

To complement the mouse modeling studies and confirm a functional role for *NF1* inactivation in human melanomas we reconstituted neurofibromin in A375 cells, which harbor compound *NF1* and $BRAF^{V600E}$ mutations. Full-length neurofibromin expression potently suppressed the growth of xenografts in mice (p=3.246E-004, Mann Whitney U test), consistent with the notion that *NF1*-inactivation plays a causal role in tumor development (Fig. 5B). As noted above, the NF1 tumor suppressor is frequently inactivated by proteasomal mechanisms in human cancer (23). As such mutational analysis may underestimate the frequency of *NF1*/neurofibromin loss in tumors. Therefore we performed immunohistochemical analysis on human melanoma tumor arrays. No visible neurofibromin expression was observed in 15% (6/39) of melanomas and 18% (6/34) of the metastatic melanomas (Fig. 5C and Supplementary Table 3). It should be noted that only a complete absence of staining was scored as negative in this analysis. Therefore excessive but incomplete neurofibromin destruction was not considered, but could still play a role in tumor development.

NF1 loss and BRAF inhibitors in human tumors

Preclinical studies in mouse tumors suggested that *Nf1* loss can desensitize *Braf* mutant melanomas to BRAF inhibitors. To evaluate this possibility in human tumors we genetically ablated neurofibromin expression with lentivrial shRNA sequences in human melanoma cell lines and found that *NF1* suppression decreased the sensitivity of WM3526 cells to PLX4720 by 11-fold (Fig. 6A and Supplementary Fig. 2). As noted previously A375 cells harbor a loss of function *NF1* mutation and express very low levels of neurofibromin. Because these cells remain somewhat sensitive to BRAF inhibitors we further reduced neurofibromin expression with shRNA sequences and found that *NF1* suppression also decreased the sensitivity of these cells to BRAF inhibitors (Fig. 6B and Supplementary Fig. 2). It should be noted that while the acute ablation of *NF1* in established melanoma cell lines desensitized these cells to PLX4720, tumors that naturally developed in the absence of *Nf1* were much more resistant to this agent. We hypothesize that this difference may reflect inherent differences in pre-existing signaling networks and/or cooperating mutations in these established tumor cells, which did not evolve in the absence of *NF1*. Nevertheless, consistent with observations in mouse tumors, PLX4720 was much less effective at suppressing phospho-ERK in cells in which NF1 was ablated, indicating that NF1 loss was promoting BRAF-independent ERK signaling in these tumor cells as well (Fig. 6C).

Finally, we were able to obtain frozen tissue from 5 sets of pre- and post-treatment tumor biopsies from patients treated with a BRAF inhibitor (vemurafenib) or combined BRAF and MEK inhibitor (dabrafenib + trametinib). Notably, 2 out of 5 tumors expressed very little or no neurofibromin prior to treatment, consistent with observation that *NF1*/neurofibromin is lost or suppressed in human melanomas at a relatively frequent rate (Fig. 6D). However in 2 of the remaining 3 tumors where neurofibromin was robustly expressed prior to treatment, neurofibromin was no longer expressed in tumors following treatment (Fig. 6D). Taken together with preclinical studies in the mouse model and genetic studies in human melanoma cell lines, these observations further support the hypothesis that *NF1*/neurofibromin suppression may play an important role in mediating resistance to BRAF inhibitors. Notably, in glioblastoma neurofibromin appears to be more frequently lost by proteasomal mechanisms (23). Therefore future studies aimed at assessing *NF1*/neurofibromin loss in response to therapies will likely require analysis of both protein expression and genetic alterations.

NF1 mutations cooperate with *BRAF* mutations by activating both K- and HRAS

Our central hypothesis is that loss of *NF1* alleviates the suppression of RAS imposed by activated BRAF. To identify the RAS isoforms that are critically regulated by neurofibromin

in melanomas we performed both gain- and loss-of-function studies. In melanoma cells that retain neurofibromin expression RNAi-mediated suppression of neurofibromin resulted in the activation of H- and KRAS, but not NRAS (Fig. 7A). Conversely, reconstituting melanoma cell lines with an active neurofibromin fragment suppressed H- and KRAS activity but not NRAS activity (Fig. 7B). Finally shRNA-mediated suppression of either *H-* or *KRAS* suppressed the ability of *NF1*-deficient melanoma cells harboring an active *BRAF* mutation to proliferate and form colonies in soft agar, whereas *NRAS*-specific shRNA sequences had no effect (Fig. 7C–E). These results suggest that neurofibromin loss/suppression activates H- and KRAS in melanomas and that both of these isoforms are critical for the tumorigenicity of these cancer cells.

As shown in Supplementary Table 1, *NF1* mutations were also detected in cells that harbored inactivating *BRAF* mutations. While the kinase activity of these BRAF proteins is compromised, they have been proposed to function as scaffolds that translocate CRAF to the membrane and promote CRAF activation downstream of KRAS (38). Notably, the oncogenic effects of these mutants are significantly enhanced in the presence of $KRAS^{G12D}$ (38). Similarly, an *NF1* mutation might be expected to function as an alternative mechanism of activating KRAS, and also potentiate the effects of these *BRAF* mutants. To evaluate the contribution of RAS isoforms in human melanomas we examined WM3629 cells. Interestingly, in addition to harboring the kinase-dead $BRAF^{D594G}$ mutation and an *NF1* deletion, this cell line also possesses an activating $NRAS^{G12D}$ mutation (39, 40). The WM3670 line similarly harbors an inactivating *BRAF* mutation, as well as *NF1* and $NRAS^{G12D}$ mutations (39, 40). Consistent with the presence of these mutations and our previous observations, NRAS, KRAS, and HRAS are all activated in WM3629 cells. Moreover, shRNA-mediated ablation of all three *RAS* isoforms, *H-, K-*, and *NRAS*, suppressed the ability of WM3629 cells to proliferate and form colonies in soft agar (Fig. 7F–H). These results further demonstrate that neurofibromin critically regulates H- and KRAS in melanomas and suggest that in the presence of *NRAS* mutations all three RAS isoforms cooperate with inactivating *BRAF* mutations to promote tumorigenesis.

DISCUSSION

This study establishes several distinct roles for *NF1* in melanomagenesis. First, our data suggest that in the presence of activating *Braf* mutations, *Nf1*-loss prevents *Braf*-induced senescence of melanocytes. In mice, this results in excessive melanocyte hyperproliferation and ultimately enhances melanoma development. Importantly, *NF1* mutations co-occur with activating *BRAF* mutations in human melanomas and neurofibromin reconstitution potently suppresses the growth of human melanoma cells as xenografts, further supporting a causal role for *NF1* loss in melanomagenesis. However, we have found that *NF1* mutations can also cooperate with inactivating *BRAF* mutations in melanomas. While these *BRAF* mutations are less common, in this setting we found that *NF1* mutations co-occur with *NRAS* mutations and that all three RAS isoforms are required for the tumorigenic properties of these cells. Thus, *NF1* mutations can contribute to melanoma development in at least two genetic settings via distinct mechanisms.

We also found that in the context of activating *BRAF* alleles *NF1* mutations contribute to tumorigenesis, in part, by promoting the activation of the PI3K/AKT/mTOR pathway. Notably, the *PTEN* tumor suppressor is commonly mutated or lost in human melanomas (41). Mouse modeling studies and human tumor analysis suggest that *BRAF* and *PTEN* mutations cooperate in melanomagenesis (14). More recently, *PTEN* loss has been shown to prevent BRAF-induced senescence in mice and in human melanocytes, further supporting the notion that co-activation of these pathways is important for preventing OIS (17). Our data demonstrate that *NF1* loss is another important mechanism by which the PI3K pathway

can become inactivated in melanomas. It should be noted however, that *NF1* and *PTEN* mutations do not appear to be mutually exclusive in melanomas. Moreover, we have found that *NF1* loss also results in the activation of multiple RAS isoforms and potentiates ERK activation independent from activating *BRAF* mutations. Taken together these observations suggest that *NF1* loss contributes to melanomagenesis by enhancing the activation of both PI3K and ERK signaling, which may be important in the context of selecting effective therapies (Model presented in Fig. 7I).

Several mechanisms have been reported to mediate the resistance of *BRAF* mutant melanomas to BRAF inhibitors (42–46). Additional mechanisms are likely to be discovered and currently one prevalent mechanism of resistance has not emerged. We have shown that *Nf1* mutations confer resistance to PLX4720 in *Braf*-mutant mouse melanomas, however these tumors are sensitive to combined MEK/mTOR inhibitors. Importantly, RNAi-mediated *NF1* suppression also decreases the sensitivity of human melanoma cell lines to BRAF inhibitors and most notably *NF1*/neurofibromin is lost in a subset of relapsing and residual tumors from patients exposed to BRAF inhibitors. The observation that *NF1* is also mutated or lost in some naive primary tumors is consistent with the hypothesis that *NF1*-inactivation may contribute to both *de novo* and acquired resistance. However, while *NF1* mutations can be detected in human melanomas, the true frequency of NF1-loss may be difficult to assess, because like PTEN and P53, the NF1 protein is frequently inactivated by proteasomal destruction (23). Immunohistochemical analysis of tumor microarrays indicates that neurofibromin expression is completely absent in 15–18% of melanomas, however a more quantitative evaluation of protein levels may be required to accurately evaluate its expression/suppression before and after drug treatment. To date, much of the resistance to BRAF inhibitors appears to be driven by events that activate ERK through mechanisms that circumvent or decrease dependency on BRAF. However, aberrant activation of the PI3K/AKT pathway has also been implicated in resistance to BRAF inhibitors (46–48). In this respect NF1 (loss) is uniquely poised, as it activates the ERK pathway through its effects on KRAS and HRAS and at the same time enhances PI3K/AKT/mTOR signaling.

METHODS

Cell Culture Techniques, Infections and Proliferation Curves

Wild-type and *NF1 null* mouse embryonic fibroblasts (MEFs) were generated as described (49). Cells were stably infected with a pBabe retroviral vector containing the 4-hydroxy tamoxifen (4-OHT) inducible estrogen receptor RAF-1 (ΔRAF:ER) construct (28). This construct is an estrogen receptor-RAF-1 fusion molecule, and contains the ligand-binding domain of the estrogen receptor fused to the activated RAF kinase domain of RAF-1. Cells were split to an equal density 16hr prior to harvesting in DMEM medium containing 1% fetal calf serum (FCS) and different concentrations of 4-OHT (0, 5, 50 or 500nM). For proliferation studies, cells were counted at seeded at a density of 25×10^4 in a 12-well format in DMEM medium containing 10% FCS and different concentrations of 4-OHT (0, 5, 50nM). Cells were counted the day after plating and every other day after until uninduced cells reached confluency. Media containing fresh 4-OHT was changed every 48hrs. The melanoma cell lines were obtained from the ATCC and the Garraway lab (46). No additional authentication was done by the authors. All melanoma cell lines were grown in RPMI medium supplemented with 10% FCS, penicillin and streptomycin. For dose-response curves, cells were seeded in triplicate in a 6-well format. Cells were counted the day after plating when PLX4720 (Calbiochem) was added as well as after 3 days when DMSO treated cells reached confluency. To allow comparison of IC50's between cell lines growth inhibition was calculated at 5 population doublings for every cell line. Neurofibromin activity was reconstituted using the previously described NF1-GAP related domain (GRD)

construct (20) or an expression vector containing full length NF1 cDNA. Neurofibromin expression was abolished using short hairpin RNA's specific to *NF1* (20).

Preparation of Protein Lysates and Western Blotting

RAS-GTP levels were detected using a RAS activation assay, following the manufacturer's instructions (EMD Millipore). Tumor lysates were homogenized and extracted with boiling 1% SDS buffer. Resulting protein lysates were quantified and run according to validated immunoblot procedures with the following antibodies: phospho-AKT (Ser473, #4060, Cell Signaling), phospho-AKT (Thr308, #9275, Cell Signaling), AKT (#9272, Cell Signaling), phospho-ERK (Thr202/Thr204, #4370, Cell Signaling), ERK (#9102, Cell Signaling), phospho-S6 (Ser235/236, #2211, Cell Signaling), S6 (#2317, Cell Signaling), NF1 (#A300-140A, Bethyl Laboratories), p120 (#G12920, Trans Labs), RAS (#05-516, Upstate), KRAS (#sc-30, Santa Cruz), HRAS (sc-520, Santa Cruz), NRAS (#sc-519, Santa Cruz) and MITF (#M3621, Dako). Immunoblots were quantified with Image J software.

Experimental Animals

Animal procedures were approved by the Center for Animal and Comparative Medicine in Harvard Medical School in accordance with the NIH Guild for the Care and Use of Laboratory Animals and the Animal Welfare Act. A breeding scheme was set up where mice carrying a conditional Nf1 allele (*Nf1*$^{flox/flox}$ mice) (30) were crossed to mice with a conditional activating mutation in *Braf* (*Braf*$^{CA/+}$ mice) (31) and a transgenic mouse strain harboring a tamoxifen (TM)-inducible Cre recombinase-estrogen receptor fusion transgene that is under the control of the melanocyte-specific tyrosinase promoter, designated *Tyr::CreER*^{T2} (32). Genotyping was performed by PCR as described for every model (30–32). To activate *Tyr::CreER* mice were treated topically with freshly prepared tamoxifen (T5648, Sigma) 2–3 months after birth. Tamoxifen (20mg/ml in 100% ethanol) was applied to a small section of skin on the shaven backs and the treatment schedule consisted of 4 treatments over 7 days. For all genotypes pigmentation levels were quantified weekly on a scale from 0 (no pigmentation) to 8 (high pigmentation). To study the contribution of the PI3K/AKT pathway in the observed hyperpigmentation phenotype in the *Tyr::CreER; Braf*$^{CA/+}$*; Nf1*$^{flox/flox}$ mice, animals were treated daily with the PI3K inhibitor GDC-0941 (150mg/kg, oral gavage) for 8 weeks after *Tyr::CreER* induction.

Xenograft Studies and Treatments

For cancer cell xenograft experiments nude mice were inoculated subcutaneously with 3×10^6 human or mouse melanoma cells. Tumor volumes were calculated by measuring length and width of the lesions and with the formula [(length) × (width)^2 × 0.52]. Murine *Nf1/Braf* mutant melanoma cells formed rapidly growing tumors. Two weeks after injection, when tumors were growing in log phase, mice were randomly divided into different treatment groups that were administered either the PI3K inhibitor GDC-0941 (150mg/kg, oral gavage (OG)), the mTOR inhibitor rapamycin (5mg/kg, intraperitoneal injection (IP)), the MEK inhibitor PD0325901 (10mg/kg, OG), the BRAF inhibitor PLX4720 (2.5mg/kg, IP) or the combination of both PD0325901 or PLX4720 and rapamycin. Mice were treated daily for 7 days.

Histology, Immunohistochemistry and SA-β-gal staining

Tissues were fixed in formalin, embedded in paraffin and stained with hematoxylin and eosin (H&E) where indicated. Standard immunohistochemistry and immunofluorescence protocols were followed for S100 (Z0311, Dako, 1:400) staining. An alkaline phosphatase staining method was used for NF1 (ab30325, Abcam, 1:300) immunohistochemistry. Antigen unmasking was performed by pressure cooking in citrate buffer (pH6). A human

melanoma tissue micorarray (ME804a, US Biomax Inc) was used for evaluation of NF1 expression in malignant and metastatic melanomas. Senescence associated (SA)-β-gal staining was performed on fresh mouse tissue. Small pieces were fixed for 30 min in 3% paraformaldehyde, incubated in SA-β-gal staining solution as described (50), and then embedded and sectioned.

NF1 Mutational analysis and Data mining

The entire *NF1* coding region of 11 human melanoma cell lines (Fig. 5A) was amplified in 5 overlapping RT-PCR fragments and used as the template for direct sequencing, essentially as described (51). Copy number analysis by multiplex ligation-dependent probe amplification (MLPA) was performed as described (52). The nomenclature of the mutations is based on *NF1* mRNA sequence NM_001042492.2, with 1 being the first nucleotide of the ATG start codon. Next, publicly available resources providing information on somatic mutations implicated in human melanoma cell lines (53, 54) and primary tumors (55–57) were mined.

Patient Samples

Patients with metastatic melanoma containing $BRAF^{V600E}$ mutation (confirmed by genotyping) were enrolled on clinical trials for treatment with a BRAF inhibitor (vemurafenib) or combined BRAF + MEK inhibitor (dabrafenib + trametinib) and were consented for tissue acquisition per IRB-approved protocol. Tumor biopsies were performed pre-treatment (day 0), at 10–14 days on treatment, and/or at time of progression if applicable. Formalin-fixed tissue was analyzed to confirm that viable tumor was present via hematoxylin and eosin (H&E) staining. Additional tissue was snap frozen and stored in liquid nitrogen.

Supplementary Material

Refer to Web version on PubMed Central for supplementary material.

Acknowledgments

We thank M. McMahon and K. Haigis for providing the $Braf^{CA/+}$ mice; and L.Chin for providing the *Tyr::CreER mice* and L. Garraway for cell lines.

Financial support: OM is a postdoctoral fellow of the Research Foundation Flanders (FWO). KC and the majority of this work was supported by the NCI (R01 CA111754) and the Ludwig Center at DF/HCC.

REFERENCES

1. Courtois-Cox S, Jones SL, Cichowski K. Many roads lead to oncogene-induced senescence. Oncogene. 2008; 27:2801–2809. [PubMed: 18193093]
2. Kuilman T, Michaloglou C, Mooi WJ, Peeper DS. The essence of senescence. Genes Dev. 2010; 24:2463–2479. [PubMed: 21078816]
3. Bartkova J, Rezaei N, Liontos M, Karakaidos P, Kletsas D, Issaeva N, et al. Oncogene-induced senescence is part of the tumorigenesis barrier imposed by DNA damage checkpoints. Nature. 2006; 444:633–637. [PubMed: 17136093]
4. Di Micco R, Fumagalli M, Cicalese A, Piccinin S, Gasparini P, Luise C, et al. Oncogene-induced senescence is a DNA damage response triggered by DNA hyper-replication. Nature. 2006; 444:638–642. [PubMed: 17136094]
5. Mallette FA, Gaumont-Leclerc MF, Ferbeyre G. The DNA damage signaling pathway is a critical mediator of oncogene-induced senescence. Genes Dev. 2007; 21:43–48. [PubMed: 17210786]

6. Narita M, Nunez S, Heard E, Narita M, Lin AW, Hearn SA, et al. Rb-mediated heterochromatin formation and silencing of E2F target genes during cellular senescence. Cell. 2003; 113:703–716. [PubMed: 12809602]
7. Courtois-Cox S, Genther Williams SM, Reczek EE, Johnson BW, McGillicuddy LT, Johannessen CM, et al. A negative feedback signaling network underlies oncogene-induced senescence. Cancer Cell. 2006; 10:459–472. [PubMed: 17157787]
8. Wajapeyee N, Serra RW, Zhu X, Mahalingam M, Green MR. Oncogenic BRAF induces senescence and apoptosis through pathways mediated by the secreted protein IGFBP7. Cell. 2008; 132:363–374. [PubMed: 18267069]
9. Acosta JC, O'Loghlen A, Banito A, Guijarro MV, Augert A, Raguz S, et al. Chemokine signaling via the CXCR2 receptor reinforces senescence. Cell. 2008; 133:1006–1018. [PubMed: 18555777]
10. Kuilman T, Michaloglou C, Vredeveld LC, Douma S, van Doorn R, Desmet CJ, et al. Oncogene-induced senescence relayed by an interleukin-dependent inflammatory network. Cell. 2008; 133:1019–1031. [PubMed: 18555778]
11. Gray-Schopfer VC, Cheong SC, Chong H, Chow J, Moss T, Abdel-Malek ZA, et al. Cellular senescence in naevi and immortalisation in melanoma: a role for p16? Br J Cancer. 2006; 95:496–505. [PubMed: 16880792]
12. Michaloglou C, Vredeveld LC, Soengas MS, Denoyelle C, Kuilman T, van der Horst CM, et al. BRAFE600-associated senescence-like cell cycle arrest of human naevi. Nature. 2005; 436:720–724. [PubMed: 16079850]
13. Garnett MJ, Marais R. Guilty as charged: B-RAF is a human oncogene. Cancer Cell. 2004; 6:313–319. [PubMed: 15488754]
14. Dankort D, Curley DP, Cartlidge RA, Nelson B, Karnezis AN, Damsky WE Jr, et al. Braf(V600E) cooperates with Pten loss to induce metastatic melanoma. Nat Genet. 2009; 41:544–552. [PubMed: 19282848]
15. Dhomen N, Reis-Filho JS, da Rocha Dias S, Hayward R, Savage K, Delmas V, et al. Oncogenic Braf induces melanocyte senescence and melanoma in mice. Cancer Cell. 2009; 15:294–303. [PubMed: 19345328]
16. Pollock PM, Harper UL, Hansen KS, Yudt LM, Stark M, Robbins CM, et al. High frequency of BRAF mutations in nevi. Nat Genet. 2003; 33:19–20. [PubMed: 12447372]
17. Vredeveld LC, Possik PA, Smit MA, Meissl K, Michaloglou C, Horlings HM, et al. Abrogation of BRAFV600E-induced senescence by PI3K pathway activation contributes to melanomagenesis. Genes Dev. 2012; 26:1055–1069. [PubMed: 22549727]
18. Bernards A, Settleman J. GAPs in growth factor signalling. Growth Factors. 2005; 23:143–149. [PubMed: 16019436]
19. Dasgupta B, Yi Y, Chen DY, Weber JD, Gutmann DH. Proteomic analysis reveals hyperactivation of the mammalian target of rapamycin pathway in neurofibromatosis 1-associated human and mouse brain tumors. Cancer Res. 2005; 65:2755–2760. [PubMed: 15805275]
20. Johannessen CM, Reczek EE, James MF, Brems H, Legius E, Cichowski K. The NF1 tumor suppressor critically regulates TSC2 and mTOR. Proc Natl Acad Sci U S A. 2005; 102:8573–8578. [PubMed: 15937108]
21. Comprehensive genomic characterization defines human glioblastoma genes and core pathways. Nature. 2008; 455:1061–1068. [PubMed: 18772890]
22. Ding L, Getz G, Wheeler DA, Mardis ER, McLellan MD, Cibulskis K, et al. Somatic mutations affect key pathways in lung adenocarcinoma. Nature. 2008; 455:1069–1075. [PubMed: 18948947]
23. McGillicuddy LT, Fromm JA, Hollstein PE, Kubek S, Beroukhim R, De Raedt T, et al. Proteasomal and genetic inactivation of the NF1 tumor suppressor in gliomagenesis. Cancer Cell. 2009; 16:44–54. [PubMed: 19573811]
24. Parsons DW, Jones S, Zhang X, Lin JC, Leary RJ, Angenendt P, et al. An integrated genomic analysis of human glioblastoma multiforme. Science. 2008; 321:1807–1812. [PubMed: 18772396]
25. Holzel M, Huang S, Koster J, Ora I, Lakeman A, Caron H, et al. NF1 is a tumor suppressor in neuroblastoma that determines retinoic acid response and disease outcome. Cell. 2010; 142:218–229. [PubMed: 20655465]

26. Bosch E, Cherwinski H, Peterson D, McMahon M. Mutations of critical amino acids affect the biological and biochemical properties of oncogenic A-Raf and Raf-1. Oncogene. 1997; 15:1021–1033. [PubMed: 9285556]
27. Zhu J, Woods D, McMahon M, Bishop JM. Senescence of human fibroblasts induced by oncogenic Raf. Genes Dev. 1998; 12:2997–3007. [PubMed: 9765202]
28. Woods D, Parry D, Cherwinski H, Bosch E, Lees E, McMahon M. Raf-induced proliferation or cell cycle arrest is determined by the level of Raf activity with arrest mediated by p21Cip1. Mol Cell Biol. 1997; 17:5598–5611. [PubMed: 9271435]
29. De Schepper S, Boucneau J, Lambert J, Messiaen L, Naeyaert JM. Pigment cell-related manifestations in neurofibromatosis type 1: an overview. Pigment Cell Res. 2005; 18:13–24. [PubMed: 15649148]
30. Zhu Y, Romero MI, Ghosh P, Ye Z, Charnay P, Rushing EJ, et al. Ablation of NF1 function in neurons induces abnormal development of cerebral cortex and reactive gliosis in the brain. Genes Dev. 2001; 15:859–876. [PubMed: 11297510]
31. Dankort D, Filenova E, Collado M, Serrano M, Jones K, McMahon M. A new mouse model to explore the initiation, progression, and therapy of BRAFV600E-induced lung tumors. Genes Dev. 2007; 21:379–384. [PubMed: 17299132]
32. Bosenberg M, Muthusamy V, Curley DP, Wang Z, Hobbs C, Nelson B, et al. Characterization of melanocyte-specific inducible Cre recombinase transgenic mice. Genesis. 2006; 44:262–267. [PubMed: 16676322]
33. Ramjaun AR, Downward J. Ras and phosphoinositide 3-kinase: partners in development and tumorigenesis. Cell Cycle. 2007; 6:2902–2905. [PubMed: 17993782]
34. Johannessen CM, Johnson BW, Williams SM, Chan AW, Reczek EE, Lynch RC, et al. TORC1 is essential for NF1-associated malignancies. Curr Biol. 2008; 18:56–62. [PubMed: 18164202]
35. Ji Z, Flaherty KT, Tsao H. Targeting the RAS pathway in melanoma. Trends Mol Med. 2012; 18:27–35. [PubMed: 21962474]
36. Bollag G, Hirth P, Tsai J, Zhang J, Ibrahim PN, Cho H, et al. Clinical efficacy of a RAF inhibitor needs broad target blockade in BRAF-mutant melanoma. Nature. 2010; 467:596–599. [PubMed: 20823850]
37. De Raedt T, Walton Z, Yecies JL, Li D, Chen Y, Malone CF, et al. Exploiting cancer cell vulnerabilities to develop a combination therapy for ras-driven tumors. Cancer Cell. 2011; 20:400–413. [PubMed: 21907929]
38. Heidorn SJ, Milagre C, Whittaker S, Nourry A, Niculescu-Duvas I, Dhomen N, et al. Kinase-dead BRAF and oncogenic RAS cooperate to drive tumor progression through CRAF. Cell. 2010; 140:209–221. [PubMed: 20141835]
39. Lin WM, Baker AC, Beroukhim R, Winckler W, Feng W, Marmion JM, et al. Modeling genomic diversity and tumor dependency in malignant melanoma. Cancer Res. 2008; 68:664–673. [PubMed: 18245465]
40. Smalley KS, Xiao M, Villanueva J, Nguyen TK, Flaherty KT, Letrero R, et al. CRAF inhibition induces apoptosis in melanoma cells with non-V600E BRAF mutations. Oncogene. 2009; 28:85–94. [PubMed: 18794803]
41. Guldberg P, thor Straten P, Birck A, Ahrenkiel V, Kirkin AF, Zeuthen J. Disruption of the MMAC1/PTEN gene by deletion or mutation is a frequent event in malignant melanoma. Cancer Res. 1997; 57:3660–3663. [PubMed: 9288767]
42. Johannessen CM, Boehm JS, Kim SY, Thomas SR, Wardwell L, Johnson LA, et al. COT drives resistance to RAF inhibition through MAP kinase pathway reactivation. Nature. 2010; 468:968–972. [PubMed: 21107320]
43. Nazarian R, Shi H, Wang Q, Kong X, Koya RC, Lee H, et al. Melanomas acquire resistance to B-RAF(V600E) inhibition by RTK or N-RAS upregulation. Nature. 2010; 468:973–977. [PubMed: 21107323]
44. Poulikakos PI, Persaud Y, Janakiraman M, Kong X, Ng C, Moriceau G, et al. RAF inhibitor resistance is mediated by dimerization of aberrantly spliced BRAF(V600E). Nature. 2011; 480:387–390. [PubMed: 22113612]

45. Shi H, Moriceau G, Kong X, Lee MK, Lee H, Koya RC, et al. Melanoma whole-exome sequencing identifies (V600E)B-RAF amplification-mediated acquired B-RAF inhibitor resistance. Nat Commun. 2012; 3:724. [PubMed: 22395615]
46. Villanueva J, Vultur A, Lee JT, Somasundaram R, Fukunaga-Kalabis M, Cipolla AK, et al. Acquired resistance to BRAF inhibitors mediated by a RAF kinase switch in melanoma can be overcome by cotargeting MEK and IGF-1R/PI3K. Cancer Cell. 2010; 18:683–695. [PubMed: 21156289]
47. Paraiso KH, Xiang Y, Rebecca VW, Abel EV, Chen YA, Munko AC, et al. PTEN loss confers BRAF inhibitor resistance to melanoma cells through the suppression of BIM expression. Cancer Res. 2011; 71:2750–2760. [PubMed: 21317224]
48. Shao Y, Aplin AE. Akt3-mediated resistance to apoptosis in B-RAF-targeted melanoma cells. Cancer Res. 2010; 70:6670–6681. [PubMed: 20647317]
49. Cichowski K, Santiago S, Jardim M, Johnson BW, Jacks T. Dynamic regulation of the Ras pathway via proteolysis of the NF1 tumor suppressor. Genes Dev. 2003; 17:449–454. [PubMed: 12600938]
50. Dimri GP, Lee X, Basile G, Acosta M, Scott G, Roskelley C, et al. A biomarker that identifies senescent human cells in culture and in aging skin in vivo. Proc Natl Acad Sci U S A. 1995; 92:9363–9367. [PubMed: 7568133]
51. Messiaen LM, Callens T, Mortier G, Beysen D, Vandenbroucke I, Van Roy N, et al. Exhaustive mutation analysis of the NF1 gene allows identification of 95% of mutations and reveals a high frequency of unusual splicing defects. Hum Mutat. 2000; 15:541–555. [PubMed: 10862084]
52. Wimmer K, Yao S, Claes K, Kehrer-Sawatzki H, Tinschert S, De Raedt T, et al. Spectrum of single- and multiexon NF1 copy number changes in a cohort of 1,100 unselected NF1 patients. Genes Chromosomes Cancer. 2006; 45:265–276. [PubMed: 16283621]
53. Barretina J, Caponigro G, Stransky N, Venkatesan K, Margolin AA, Kim S, et al. The Cancer Cell Line Encyclopedia enables predictive modelling of anticancer drug sensitivity. Nature. 2012; 483:603–607. [PubMed: 22460905]
54. Forbes SA, Bindal N, Bamford S, Cole C, Kok CY, Beare D, et al. COSMIC: mining complete cancer genomes in the Catalogue of Somatic Mutations in Cancer. Nucleic Acids Res. 2011; 39:D945–D950. [PubMed: 20952405]
55. Berger MF, Hodis E, Heffernan TP, Deribe YL, Lawrence MS, Protopopov A, et al. Melanoma genome sequencing reveals frequent PREX2 mutations. Nature. 2012; 485:502–506. [PubMed: 22622578]
56. Hodis E, Watson IR, Kryukov GV, Arold ST, Imielinski M, Theurillat JP, et al. A landscape of driver mutations in melanoma. Cell. 2012; 150:251–263. [PubMed: 22817889]
57. Krauthammer M, Kong Y, Ha BH, Evans P, Bacchiocchi A, McCusker JP, et al. Exome sequencing identifies recurrent somatic RAC1 mutations in melanoma. Nat Genet. 2012; 44:1006–1014. [PubMed: 22842228]

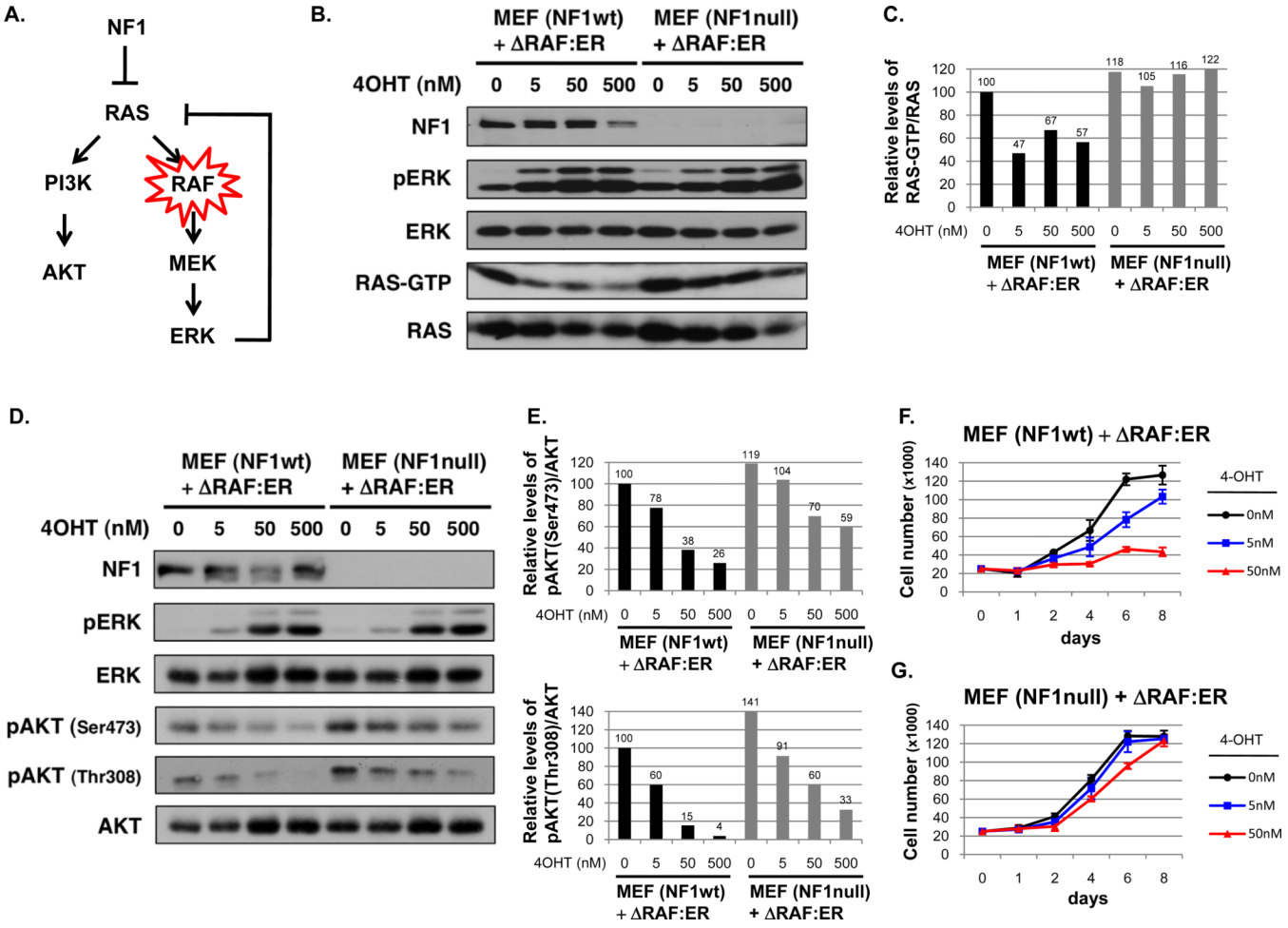

Figure 1. *NF1* mutations rescue the inhibitory effects of activated RAF

A) Model of negative feedback pathway and the role that NF1 could play in alleviating suppression. **B)** *NF1* wild-type (wt) and null mouse embryonic fibroblasts (MEFs) expressing an inducible RAF construct (ΔRAF:ER) were treated with the indicated concentrations of hydroxy-tamoxifen (4-OHT) for 24 hours. Immunoblots of total cell lysates evaluating phospho-ERK, total ERK, RAS, and neurofibromin (NF1) are shown. RAS-GTP levels were assessed using a RAS pull-down assay and are quantified relative to total RAS levels in panel **C**. **D)** Immunoblots evaluating phospho-ERK and phospho-AKT in total cell lysates from cells treated with 4-OHT for 72 hours are shown. Relative phospho-AKT (Ser473) and phospho-AKT (Thr308) levels are quantified in panel **E**. **F)** Proliferation curve of *NF1* wt and **G)** *NF1* null MEFs expressing the inducible RAF construct after exposure to increasing concentrations of 4-OHT.

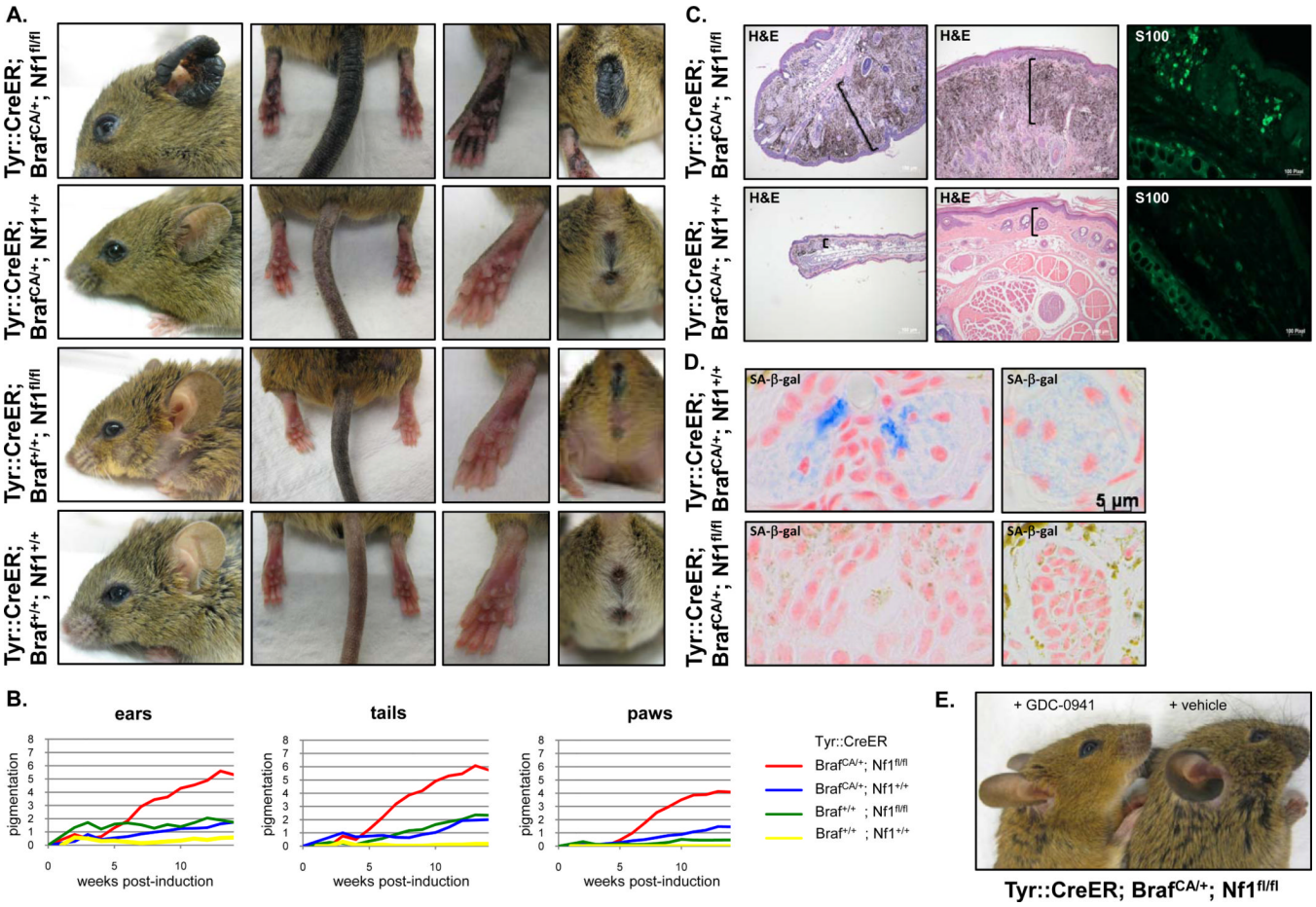

Figure 2. *Nf1* and *Braf* mutations cooperate *in vivo* and lead to enhanced melanocyte proliferation

A) Phenotype of mice with the indicated genotypes 7 months after *Tyr::CreER* induction. **B)** Quantification of pigmentation phenotype of different genotypes over time following *Tyr::CreER* induction. **C)** Histological images of ears (left panels) and tails (middle panels) from mice with the specified genotypes 9 months after tamoxifen treatment. S100 expression was evaluated by immunofluorescent staining (right panels). **D)** Sections of ear stained for eosin and senescence-associated (SA)-β-galactosidase (light blue) from tamoxifen treated *Tyr::CreER; Braf*$^{CA/+}$*; Nf1*$^{+/+}$ (top panel) and *Tyr::CreER; Braf*$^{CA/+}$*; Nf1*$^{flox/flox}$ mice (bottom panel) mice. Note the blue staining and cell morphology differences. **E)** *Tyr::CreER; Braf*$^{CA/+}$*; Nf1*$^{flox/flox}$ mice were treated daily with the PI3K inhibitor GDC-0941 (150mg/kg) or vehicle for 8 weeks after *Tyr::CreER* induction. The hyperpigmentation phenotype was prevented by GDC-0941 treatment.

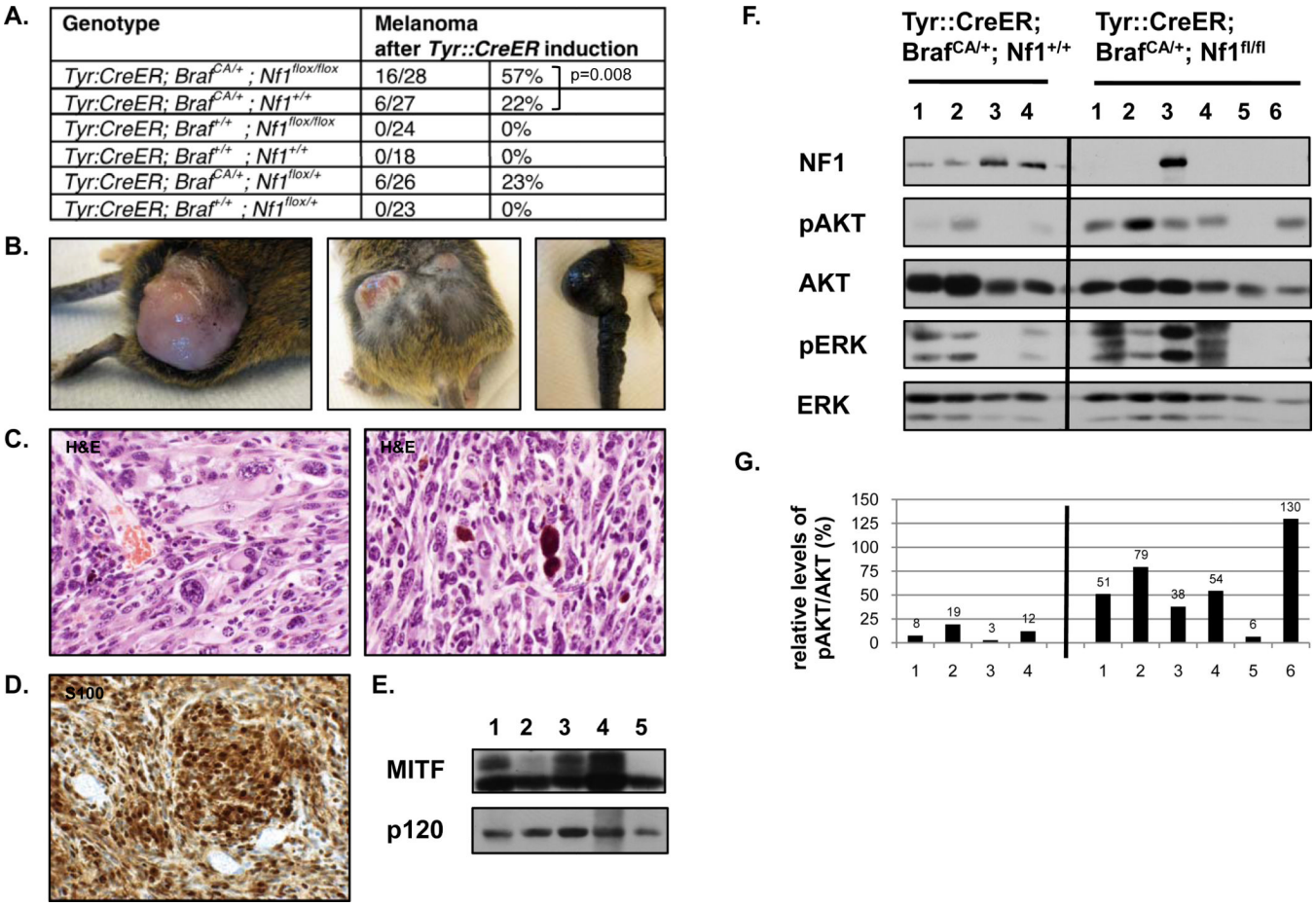

Figure 3. *Nf1* and *Braf* mutations cooperate to promote melanomagenesis in mice

A) Genotypes and tumor phenotypes of experimental animals and control groups. **B)** Pictures showing tumors from tamoxifen (TM) treated *Tyr::CreER; Braf$^{CA/+}$; Nf1$^{flox/flox}$* mice. Note the pigmented area on the surface of the tumor (left panel), the presence of more than one lesion (middle panel) and the remarkable thickening of the tail (right panel). **C–D)** Representative histological images (400× magnification) of tumors from TM-induced *Tyr::CreER; Braf$^{CA/+}$; Nf1$^{flox/flox}$* mice. **C)** Tumor sections are stained with hematoxylin and eosin (H&E). Tumors show marked cytologic atypia and pleomorphism, including bizarre cells, with irregular chromatin distribution and irregular nuclear outlines (left panel). Occasionally, melanophages containing extensive brown pigment were observed (right panel). **D)** The vast majority of neoplastic cells stain positive for S100. **E)** MITF protein expression in primary tumor tissue from TM-treated *Tyr::CreER; Braf$^{CA/+}$; Nf1$^{flox/flox}$* mice was confirmed by immunoblotting. **F)** Protein levels of NF1, phospho-AKT and phospho-ERK in distinct tumors from TM-induced *Tyr::CreER; Braf$^{CA/+}$; Nf1$^{+/+}$* (left) and *Tyr::CreER; Braf$^{CA/+}$; Nf1$^{flox/flox}$* (right) mice, as determined by immunoblotting. Relative phospho-AKT levels are quantified in panel **G**.

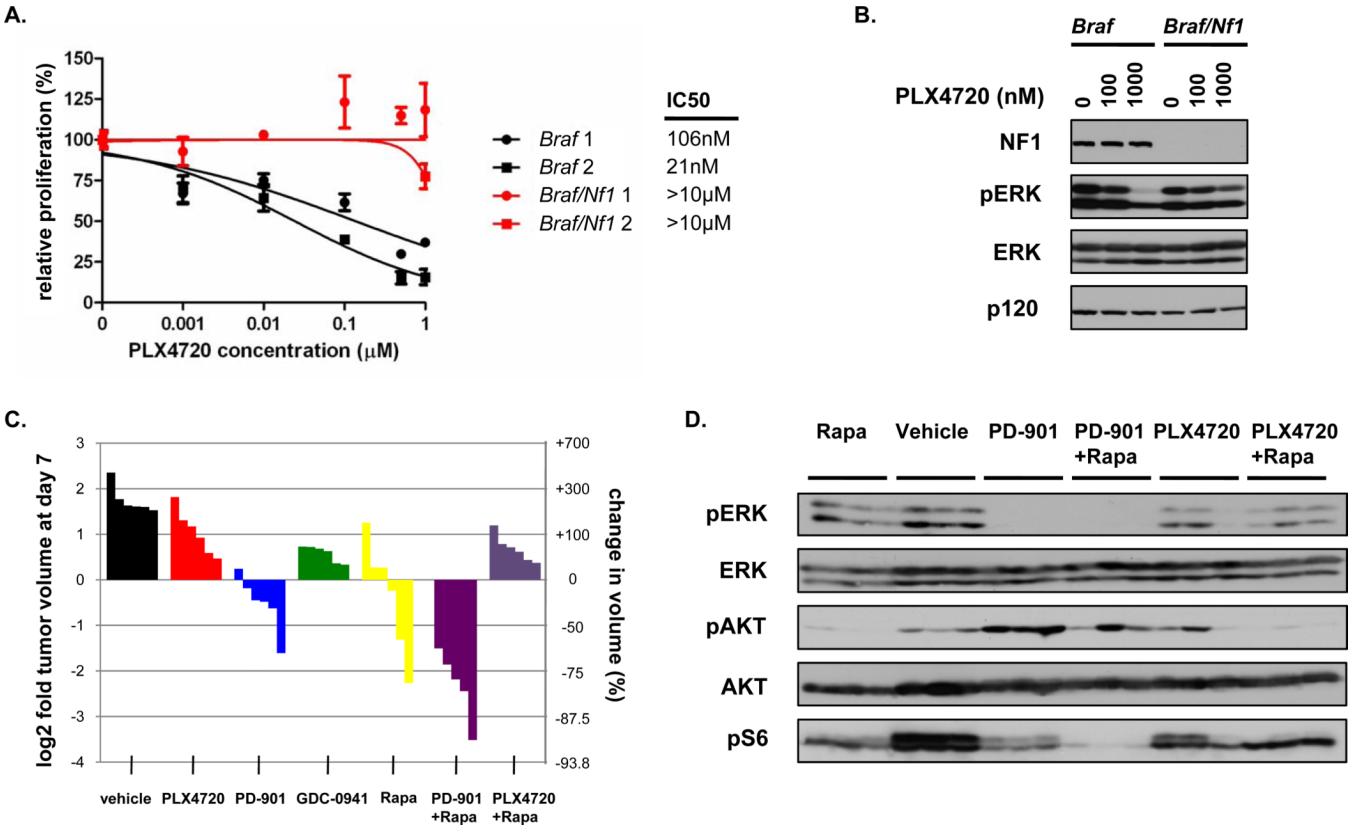

Figure 4. *Nf1* mutations densensitize mouse melanomas to BRAF inhibitors

A) Dose sensitivity curves for PLX4720 are shown for two independently derived cell lines from *Braf* mutant (black) and *Braf/Nf1* mutant (red) melanomas. **B)** Pharmacodynamic analysis of phospho-ERK in *Braf* and *Braf/Nf1* cells *in vitro* after a 24-hour incubation with 0, 100, and 1000nM PLX4720. **C)** Waterfall plot depicting tumor growth of *Braf/Nf1* mutant allografts after 7 days of treatment with vehicle (black), PLX4720 (red), PD0325901 (blue), GDC-0941 (green), rapamycin (yellow), PD0325901/rapamycin (purple), and PLX4720/rapamycin (violet). Each bar represents a different tumor. Both *Braf/Nf1* mutant cell lines shown in Fig. 4A were injected into three mice each, resulting in a total of 6 tumors per treatment arm. **D)** *In vivo* pharmacodynamic analysis of phospho-ERK, phospho-AKT, and phospho-S6 in *Braf/Nf1* mutant allografts treated with Rapamycin (Rapa), Vehicle, PD0325901 (PD-901), PD0325901/Rapamycin, PLX4720, and PLX4720/ Rapamycin. Lysates were prepared from tumor tissues that were harvested 2 hours post administration of the respective treatment from 3 tumors shown in Fig. 4C.

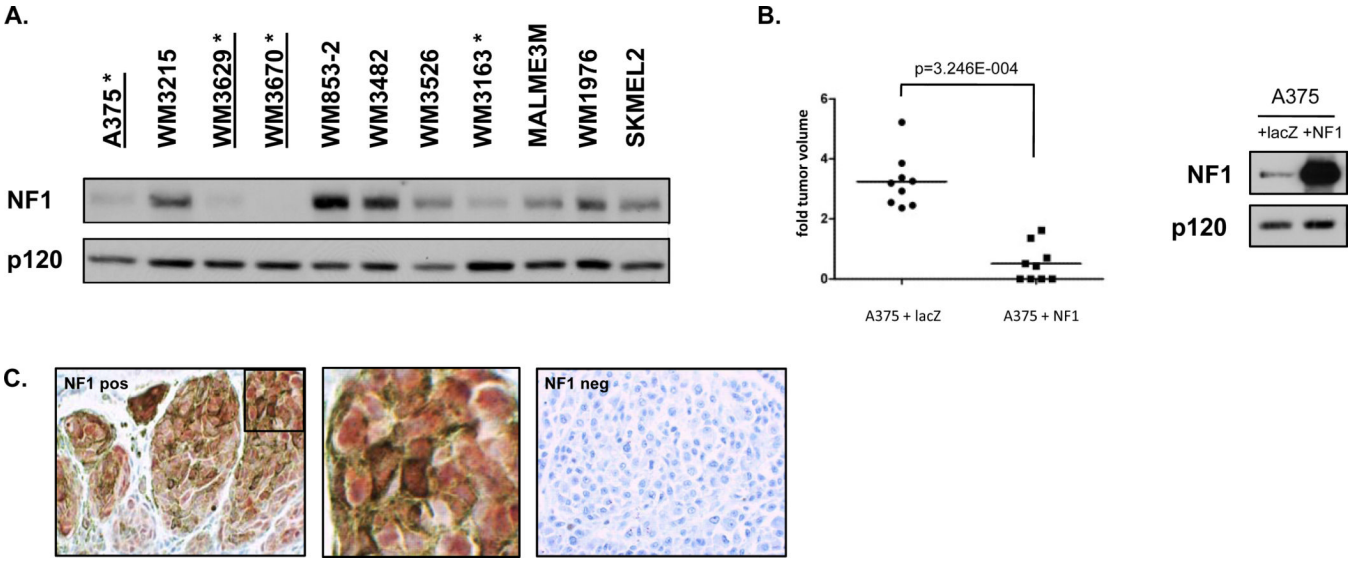

Figure 5. *NF1* protein expression in human melanomas

A) NF1 protein levels in a panel of 11 human melanomas cell lines as determined by immunoblotting. Four lines (with asterisks) exhibit low or no NF1 expression. Three lines (underlined) harbor *NF1* mutations. **B)** NF1 reconstitution in A375 cells potently suppresses the growth of xenografts in mice. Tumor size is shown on left, protein expression in right panel. **C)** Tissue microarray analysis of NF1 in human malignant and metastatic melanomas. Positive NF1 staining in nevus is shown in left panel. A magnification of the inset box is shown in the middle panel. Negative NF1 staining in human melanoma is shown in the right panel.

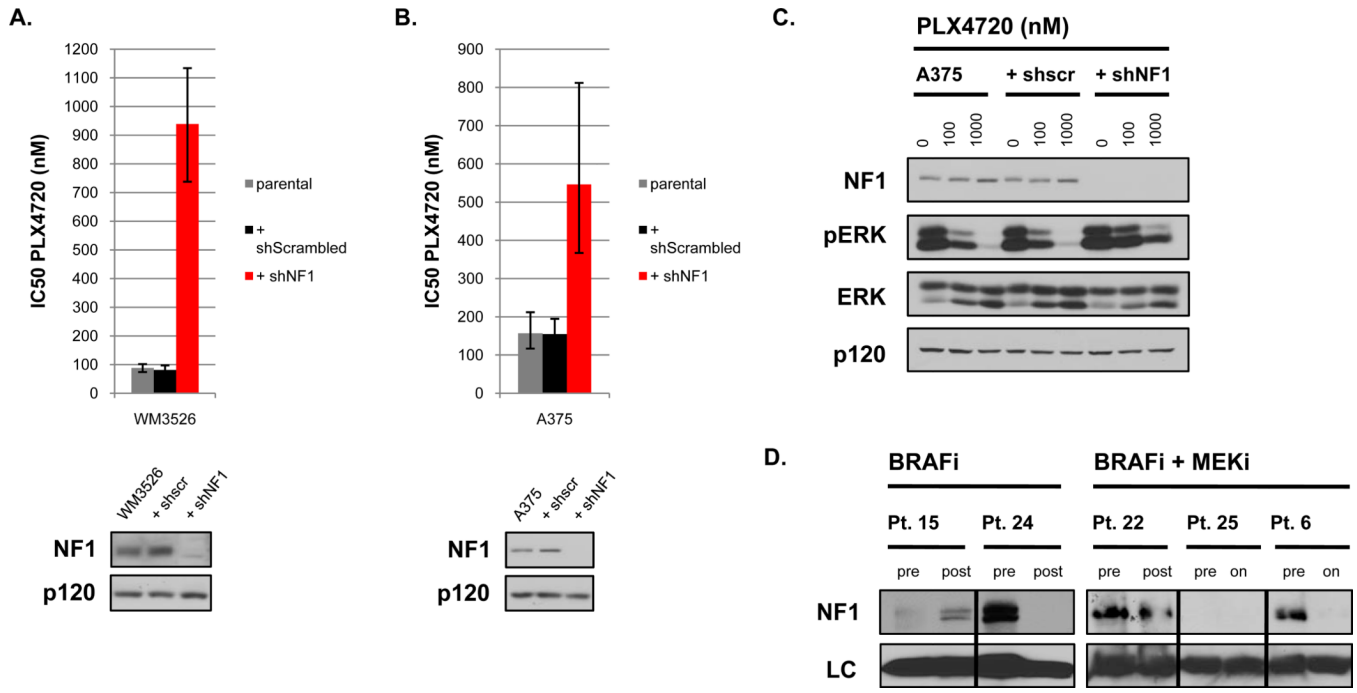

Figure 6. NF1 levels mediate sensitivity to BRAF inhibition

A) Bar graph representing IC50 values for PLX4720 in the *BRAF*^{V600E} mutant melanoma cell line WM3526 in the absence or presence of a short hairpin RNA (shRNA) specific for *NF1*. The doubling time of these cells did not change in the presence of shRNA sequences. **B)** A similar graph representing IC50 values for PLX4720 in the *BRAF*^{V600E} mutant melanoma cell line A375. **C)** Pharmacodynamic analysis of phospho-ERK in A375 cells with or without residual NF1 expression after a 24-hour incubation with 0, 100, and 1000nM PLX4720. **D)** NF1 protein levels in tumor biopsies from patients (Pt.) before and after treatment with a BRAF inhibitor (BRAFi) (vemurafenib) or combined BRAF/MEK inhibitors (BRAF/MEKi) (dabrafenib + trametinib). Where indicated samples were collected from relapsed biopsies (post) or from residual tumor tissue while patients were still on treatment (on). Total levels of GAPDH (BRAFi samples) and HSC70 (BRAF/MEKi samples) served as loading controls (LC).

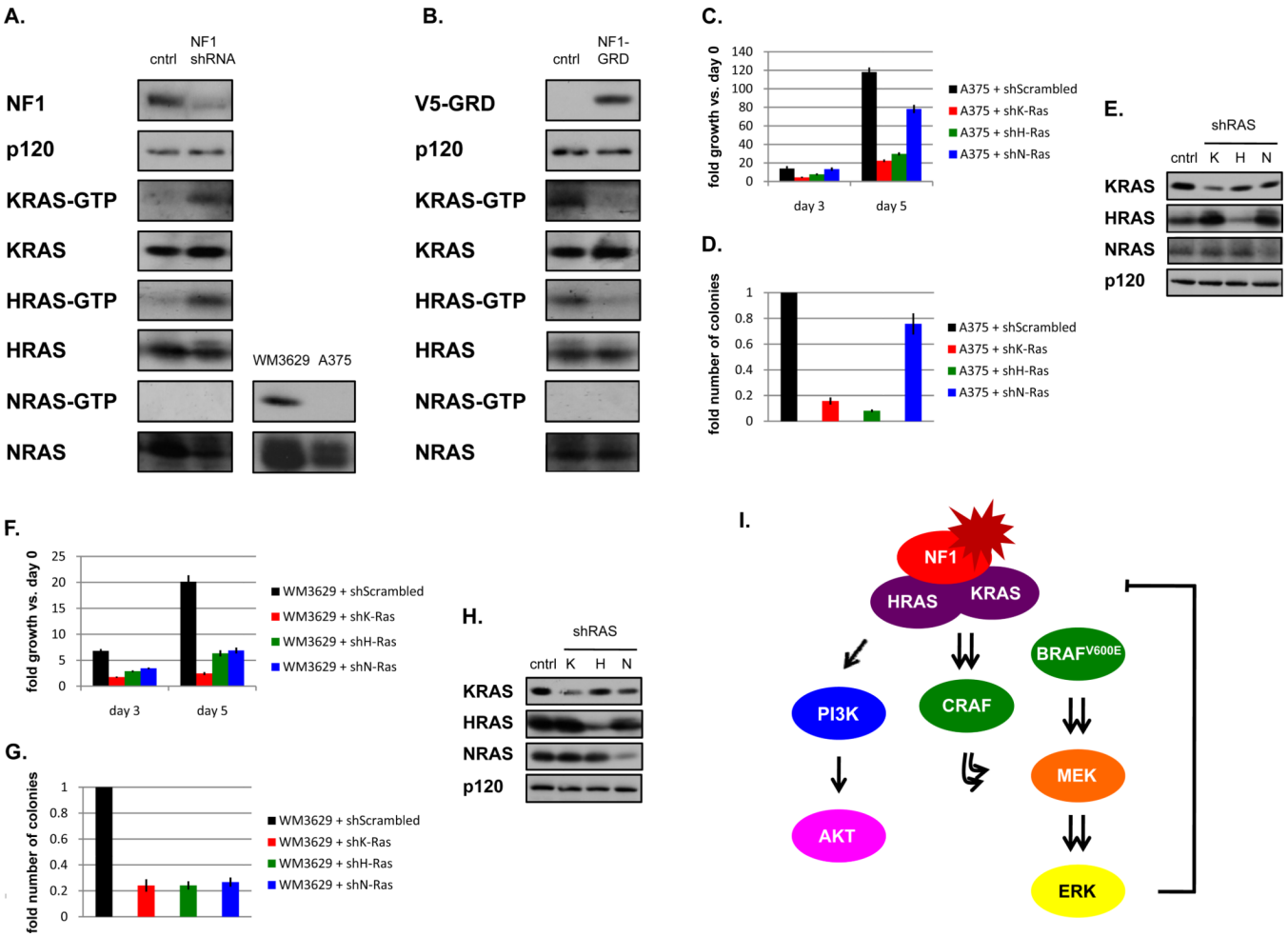

Figure 7. NF1 critically regulate KRAS and HRAS in melanomas

A) (left) In WM1976 melanoma cells that retain NF1 expression, RNAi mediated suppression of *NF1* results in the activation of H- and KRAS, but not NRAS. (bottom right panels) NRAS-GTP assay confirming that NRAS is active in melanoma cells with an activating *NRAS* mutation (WM3629), but not in melanoma cells wild-type for NRAS (A375). **B)** Ectopic expression of the catalytically active NF1 fragment (GAP-related domain, GRD) suppresses H- and KRAS, but not NRAS activity in melanoma cells (MALME3M). RAS-GTP levels were assessed using a RAS pulldown assay. Immunoblots on total cell lysates are shown. **C)** shRNA mediated suppression of *H-* or *KRAS*, but not *NRAS*, suppresses the ability of A375 cells to proliferate and **D)** form colonies in soft agar. **E)** Confirmation of RAS isoform-specific knockdown by shRNAs in A375 cells. **F)** shRNA mediated suppression of *H-*, *K-* and *NRAS* suppresses the ability of WM3629 cells to proliferate and **G)** form colonies in soft agar. **H)** Confirmation of RAS isoform-specific knockdown by shRNAs in WM3629 cells. **I)** Suggested model for the distinct roles of NF1 in melanomagenesis.